Abs. 288, 206th Meeting, © 2004 The Electrochemical Society, Inc.

Comparative Study of Li[$Ni_{1/2}Mn_{3/2}$]O_4 (*P*$4_3$32) and Li[$Ni_{1/2}Mn_{3/2}$]O_4 (*Fd*3*m*) for Advanced Lithium-Ion Batteries

Kingo Ariyoshi and Tsutomu Ohzuku
Graduate School of Engineering, Osaka City University
(OCU) Osaka 558-8585, Japan

Noriaki Nakayama
Faculty of Engineering, Yamaguchi University
Ube 755-8611, Japan

In a previous paper [1], we have reported solid state chemistry and electrochemistry of Li[$Ni_{1/2}Mn_{3/2}$]O_4 (*P*$4_3$32) having a superlattice structure. This sample shows extremely flat operating voltage of 4.75 V and the reaction consists of two topotactic two-phase reactions. We prepared Li[$Ni_{1/2}Mn_{3/2}$]O_4 (*P*$4_3$32) sample by a two-step solid-state reaction [2-4]. However, one-step solid-state reaction also gives approximate Li[$Ni_{1/2}Mn_{3/2}$]O_4 having rechargeable capacities more than 120 mAh/g in voltages of 3.0 to 4.9 V. In this study we show the effect of formation of superlattice on lithium insertion scheme.

Two types of Li[$Ni_{1/2}Mn_{3/2}$]O_4 are prepared from LiOH and nickel manganese double hydroxides (MX-003-2 or MX-008-3). One is prepared by heating a reaction mixture at 1000°C and then cooling down to room temperature. Another is prepared by a two-step solid-state reaction, *i.e.*, oxidation at 700°C followed by crystal growth at 1000°C. XRD and electron diffraction examinations indicate that the former is identified as normal spinel of *Fd*3*m* and the latter as a superlattice structure of *P*$4_3$32.

Figure 1 shows the FT-IR spectra of two types of Li[$Ni_{1/2}Mn_{3/2}$]O_4. Li[Mn_2]O_4 (*Fd*3*m*) is also shown in Fig. 1. As can be seen in Fig 1(b), IR spectrum of Li[$Ni_{1/2}Mn_{3/2}$]O_4 (*Fd*3*m*) is classified at somewhere between Li[$Ni_{1/2}Mn_{3/2}$]O_4 (*P*$4_3$32) and Li[Mn_2]O_4(*Fd*3*m*). Figure 2 shows the charge and discharge curves of Li / Li[$Ni_{1/2}Mn_{3/2}$]O_4 cells. Li[$Ni_{1/2}Mn_{3/2}$]O_4 (*P*$4_3$32) shows extremely flat operating voltage of *ca.* 4.75 V as was already reported[1]. Li[$Ni_{1/2}Mn_{3/2}$]O_4 (*Fd*3*m*) shows the rechargeable capacity of ca. 125 mAh/g. As seen in Fig. 2, sloping operating voltage especially in 3.8 to 4.6 V is characteristic of Li[$Ni_{1/2}Mn_{3/2}$]O_4 (*Fd*3*m*). Difference in rechargeable capacity is about 15 mAh/g between two samples.

Figure 3 shows the change in cubic lattice constant as a function of x in Li_{1-x}[$Ni_{1/2}Mn_{3/2}$]O_4 (*Fd*3*m*). Lattice constant decreased linearly from 8.18 to 8.08 Å in x = 0 to 0.5. In x > 0.5, two cubic phases coexisted, *i.e.*, 8.08 and 8.01 Å.

From these results, we will show the differences and similarities between Li[$Ni_{1/2}Mn_{3/2}$]O_4 (*P*$4_3$32) and Li[$Ni_{1/2}Mn_{3/2}$]O_4 (*Fd*3*m*) in relation to preparation conditions and discuss topotactic two-phase versus one-phase reaction with emphasis on superlattice formation.

References

[1] K. Ariyoshi, Y. Iwakoshi, N. Nakayama, and T. Ohzuku, *J. Electrochem. Soc.*, **151**, A296(2004).
[2] T. Ohzuku, K. Ariyoshi, S. Yamamoto, and Y. Makimura, *Chemistry Letters*, **30**, 1270(2001).
[3] T. Ohzuku, K. Ariyoshi, and S. Yamamoto, *J. Ceramic Soc. Jpn.*, **110**, 501(2002).
[4] K. Ariyoshi, S. Yamamoto, and T. Ohzuku, *J. Power Sources*, **119-121**, 959(2003).

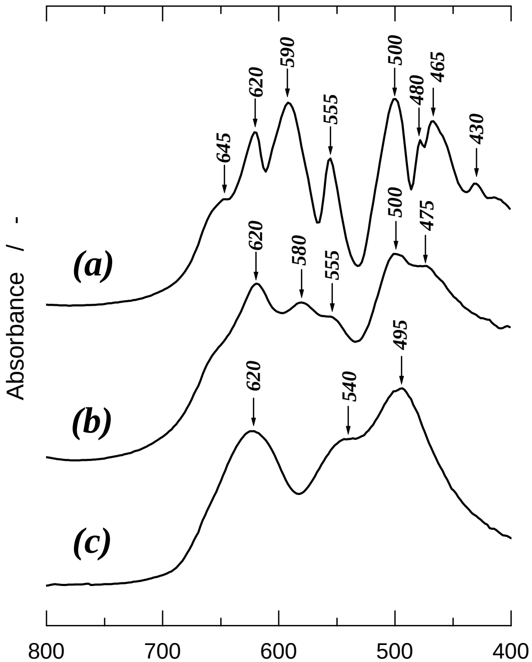

Fig. 1 FT-IR spectra of (a) Li[$Ni_{1/2}Mn_{3/2}$]O_4 (*P*$4_3$32) and (b) Li[$Ni_{1/2}Mn_{3/2}$]O_4 (*Fd*3*m*). FT-IR spectrum of $LiMn_2O_4$ is also shown in (c) for comparison.

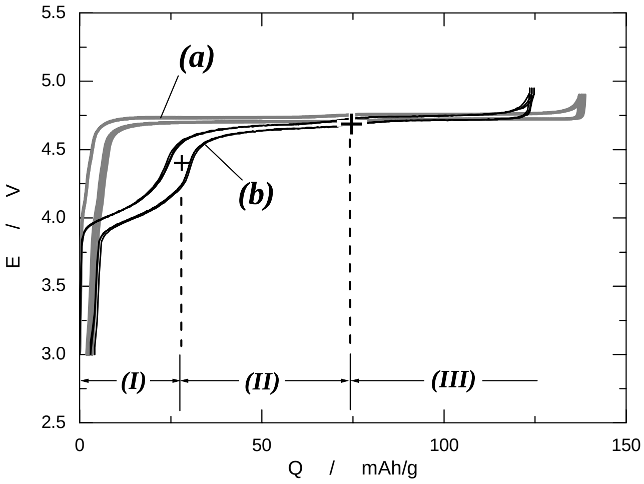

Fig. 2 Charge and discharge curves of lithium cells with (a) Li[$Ni_{1/2}Mn_{3/2}$]O_4 (*P*$4_3$32) and (b) Li[$Ni_{1/2}Mn_{3/2}$]O_4 (*Fd*3*m*). The cells were operated at a rate of 0.17 mA/cm^2 at 30°C. The electrolyte used was 1 M $LiPF_6$ dissolved in EC / DMC (3/7 by volume).

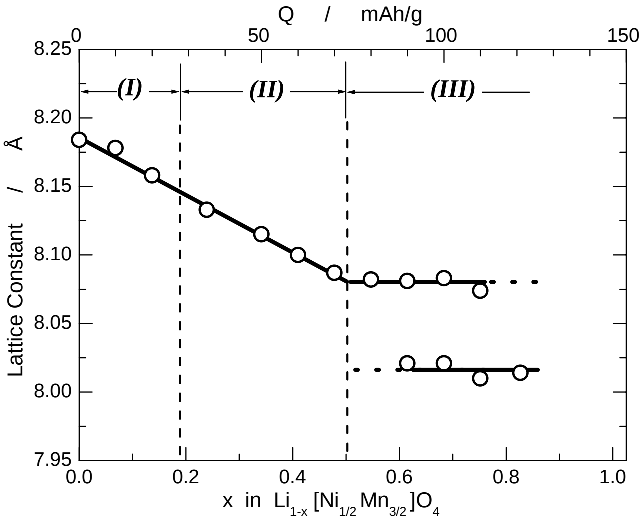

Fig. 3 Change in lattice constant as a function of x in Li_{1-x}[$Ni_{1/2}Mn_{3/2}$]O_4 (*Fd*3*m*).